

Laser damage resistance of hafnia thin films deposited by electron beam deposition, reactive low voltage ion plating, and dual ion beam sputtering

Laurent Gallais,* Jérémie Capoulade, Jean-Yves Natoli, Mireille Commandré, Michel Cathelinaud, Cian Koc, and Michel Lequime

Institut Fresnel (UMR CNRS 6133), Université Paul Cezanne, Université de Provence - Ecole Centrale Marseille Domaine Universitaire de St Jérôme, 13397 Marseille Cedex 20, France

*Corresponding author: laurent.gallais@fresnel.fr

Received 6 August 2007; accepted 17 September 2007;
posted 10 October 2007 (Doc. ID 85810); published 29 November 2007

A comparative study is made of the laser damage resistance of hafnia coatings deposited on fused silica substrates with different technologies: electron beam deposition (from Hf or HfO₂ starting material), reactive low voltage ion plating, and dual ion beam sputtering. The laser damage thresholds of these coatings are determined at 1064 and 355 nm using a nanosecond pulsed YAG laser and a one-on-one test procedure. The results are associated with a complete characterization of the samples: refractive index n measured by spectrophotometry, extinction coefficient k measured by photothermal deflection, and roughness measured by atomic force microscopy. © 2008 Optical Society of America
OCIS codes: 310.0310, 140.3330.

1. Introduction

HfO₂ is one of the most important high index materials for the production of optical multilayer coatings for UV to IR applications. In addition to its good optical and mechanical properties, HfO₂ is also known for its high laser-induced damage threshold (LIDT). It has been shown through different studies [1-5] that hafnia coatings with very high laser damage threshold from the deep ultraviolet (DUV) to the IR can be produced by electron beam evaporation. In this case the best thresholds for hafnia have been obtained by reactive evaporation of hafnium. Indeed it has been shown that, when optimized, this technique reduces the number of defects [1,4] compared to evaporation from HfO₂. However, coatings produced with these technologies are rather porous and cannot be used for very demanding applications where multilayer coatings with complex spectral characteristics are to be produced. On the contrary, the use of plasma or ion assistance during deposition produces films

with densities approaching that of the bulk material, with larger refractive index, better mechanical and structural properties, and less effect by the environment [6,7]. But for these last technologies, the laser damage resistance is still a key limitation [8,9].

The improvement of the laser damage resistance of dense layers has therefore a considerable interest for the community. As a consequence, in an effort to produce multilayer coatings for high power applications, we present a comparative study of the laser damage resistance of hafnia coatings deposited with different assisted and unassisted deposition techniques. These coatings have been produced with the optimized process developed at the Fresnel Institute for this material. The work presented in this paper follows a first study made on a low index material (silica) [10].

In Section 2 a description of the different produced samples is given, along with the process parameters used for deposition. In Section 3 the results of the nondestructive characterizations are given. In Section 4 the experimental setup and procedures for laser-damage testing are described and the results

are presented. This is followed by a discussion in Section 5 on the obtained laser damage thresholds.

2. Samples Preparation

A. Samples Description

The substrate choice and preparation (cleaning and polishing) are critical for the production of coatings for high power applications, and they can ultimately limit the thresholds for a given coating [11,12]. For this study we used 1 in. (2.5 cm) diameter fused silica substrates (Corning 7980) polished for high power applications. All the substrates come from the same batch and have been polished at the same time.

To clean these substrates, we used an automatic aqueous cleaning procedure, involving ultrasonic immersion and detergents followed by deionized water rinsing and drying.

The samples were prepared by electron beam deposition using either a hafnium or hafnia source (respectively, the samples are called EBD-Hf or EBD-HfO₂ in the following text), reactive low voltage ion plating (RLVIP), and dual ion beam sputtering (DIBS). Hafnia being a material that can be used in the UV or IR region, our aim was to test them at 355 and 1064 nm (first and third Nd:YAG harmonics). However, to have comparable results at a given wavelength, it is necessary to ensure that the optical thicknesses of the different samples are the same, in order to have the same standing electric field in the coating. Then, a first series of samples, half-wave at 1064 nm, was made for testing at 1064 nm and a second series, half-wave at 355 nm, was made for 355 nm testing. Two samples were made for each thickness: one for the laser damage tests and one for the nondestructive characterizations, in order to avoid contamination effects before measurements. A bare substrate was also associated with each deposition technique (i.e., cleaned and stocked in the same conditions) and laser-damage tested.

To summarize, the samples and their denomination used in this paper are referenced in Table 1.

Table 1. Sample Labels

Reference	Deposition Technique	Optical Thickness
DIBS 2H at 1064 nm	Dual ion beam sputtering	$\lambda/2$ at 1064 nm
DIBS 2H at 355 nm	Dual ion beam sputtering	$\lambda/2$ at 355 nm
RLVIP 2H at 1064 nm	Reactive low voltage ion plating	$\lambda/2$ at 1064 nm
RLVIP 2H at 355 nm	Reactive low voltage ion plating	$\lambda/2$ at 355 nm
EBD-Hf 2H at 1064 nm	EBD from an hafnium source	$\lambda/2$ at 1064 nm
EBD-Hf 2H at 355 nm	EBD from an hafnium source	$\lambda/2$ at 355 nm
EBD-HfO ₂ 2H at 1064 nm	EBD from an hafnia source	$\lambda/2$ at 1064 nm
EBD-HfO ₂ 2H at 355 nm	EBD from an hafnia source	$\lambda/2$ at 355 nm

B. Deposition Procedures

The equipment used for electron beam deposition (EBD) and ion plating is a Balzers BAP 800 reactive ion plating system. This equipment and its configuration are described in more detail in Ref. [13]. The chamber contains two crucibles heated by electron-beam guns and a source of argon plasma used in the ion plating process. In the absence of use of this source, the layers are obtained through a standard EBD process. The rate of evaporation during the deposition is controlled by a quartz-crystal monitor, and the optical thicknesses of the layers are controlled by an *in situ* optical monitoring system. The EBD layers were deposited using either a hafnium or a hafnia starting material. The RLVIP samples were made from a hafnium starting material.

Teers Coating equipment was used for the dual ion beam sputtering process. With this technique, a first ion source is used for sputtering a plane target (hafnium), and a second ion source is directed toward the substrates for providing argon ions, whose energy is used to compact the layer material. The vacuum chamber is also equipped with quartz-thickness-controller and *in situ* optical monitoring.

The different parameters used for these experiments are reported in Table 2 (the same parameters were used for the layers $\lambda/2$ at 355 nm and $\lambda/2$ at 1064 nm).

3. Nondestructive Characterizations

A. Refractive Index

The film's transmittance and reflectance spectra were measured with a Lambda 18 PerkinElmer spectrophotometer, in order to calculate the refractive index n . The n value is obtained by fitting the R and T measurements with a numerical method.

The determined refractive-index dispersion curves are plotted in Fig. 1, and the refractive indices at 355 and 1064 nm are compared in Fig. 2. These values have been measured on the thickest films ($\lambda/2$ at 1064 nm).

The RLVIP film exhibits the larger refractive index, which is very close to the bulk value reported for hafnia [14]. The refractive index value being an indication of the film density, films with bulk density are obtained with this technology. Similar results were found for EBD-Hf and EBD-HfO₂ technologies. These evaporated films have the lowest refractive index, due to their reduced density (linked to the porous structure), as commonly observed. The DIBS films are intermediate between these two behaviors.

B. Extinction Coefficient

Optical absorption is a limiting factor for laser damage resistance of optical coatings. The extinction coefficient k is a good indication of the coating quality; it is associated with nonstoichiometry, defects, and contaminations. However, in the case of low-loss optical coatings, this value cannot be determined directly by reflectance and transmittance measurements. With this technique the loss measurements

Table 2. Process Parameters

Procedure	Deposition Technique			
	EBD-Hf	EBD-HfO ₂	RLVIP	DIBS
Starting material	Hafnium 99.5% Umicore granulate 1–10 mm	HfO ₂ tablets Merck Patinal	Hafnium 99.5% Umicore granulate 1–10 mm	Hafnium 99.4% Neyco
Liner	Carbon	Molybdenum	Carbon	
Evaporation gun	10 kV	10 kV		1 kV, 400 mA, acceleration: 350 V
Assistance parameters			Plasma source arc current and voltage: 55 A, 66 V Anode voltage: 42 V	Ion gun: 375 V, 350 mA acceleration: 300 V
Base pressure	3×10^{-7} mbar	3×10^{-7} mbar	3×10^{-7} mbar	7×10^{-7} mbar
Chamber pressure	5×10^{-4} mbar (O ₂)	5×10^{-4} mbar (O ₂)	6×10^{-4} mbar (Ar + O ₂)	5.5×10^{-4} mbar (Ar + O ₂)
Deposition rate	0.9 nm/s	0.9 nm/s	0.2 nm/s	0.05 nm/s
Substrate temperature	250 °C lamp heaters	250 °C lamp heaters	200–250 °C no heaters	50 °C no heaters
Anode voltage			42 V	

are limited to 10^{-3} , and scattering losses cannot be separated from absorption losses. The photothermal deflection technique is an adequate method for measuring absorption losses in the 10^{-4} – 10^{-7} range [15]. Furthermore, the extinction coefficient k can be calculated from the absorption measurement, knowing the refractive index n and thickness.

To measure our samples, we used the photothermal deflection setup described in Ref. [16]. The pump beam was a cw argon laser (Spectra Physics 2065-7S Beamlock) tuned to operate in the mid-UV argon lines (333.6–363.8 nm). The beam was modulated at 1500 Hz and focused on the sample with a 15 μm beam diameter (diameter at $1/e^2$). The probe beam was a He–Ne laser working in the transmission configuration.

With this technique, calibration is needed to obtain the absorption value from the measurement of the deflection signal. We performed calibration by comparing the deflection caused by the absorption of the sample with that of a sample of known absorption. In this case it was titanium-implanted silica substrates, having the same thermal properties as the samples under test. The validity of this calibration procedure

has been shown in Ref. [17]. The lowest measurable absorptance that could be detected was 10^{-7} .

The mean absorption was measured with this setup on the different samples. The extinction coefficient was then obtained, assuming bulk absorption in the layer and neglecting interfacial absorption, by using the relation between the absorption A and k [18]:

$$A = \frac{4\pi k}{\lambda} \frac{n}{n_0} \int_0^e \left| \frac{E(z)}{E_{inc}} \right|^2 dz, \quad (1)$$

with n as the refractive index of the layer determined previously, e as the layer thickness, n_0 as the air refractive index, $E(z)$ as the electric field in the layer as a function of the depth z , and E_{inc} as the incident electric field. The results obtained with this method are plotted in Fig. 3. These results are linked to the damage measurements in Section 5.

C. Roughness

The surface roughness was measured with an atomic force microscope (Quesant Q-scope 250). We used the contact mode imaging with a scanned area of

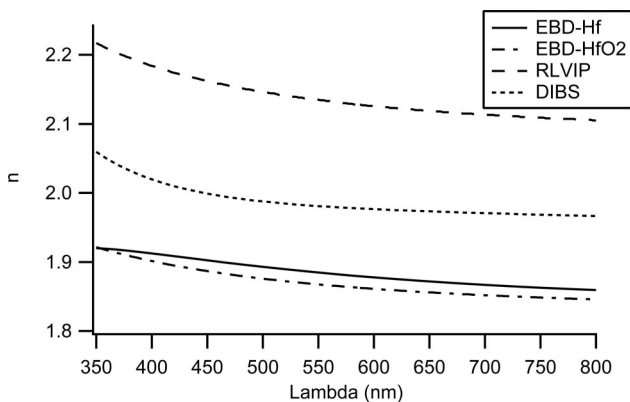


Fig. 1. Refractive index dispersion curves.

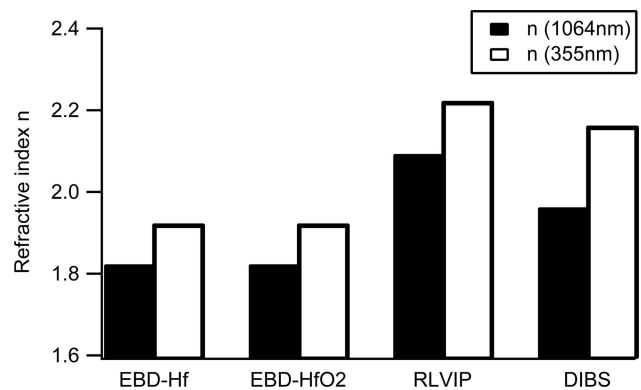


Fig. 2. Refractive index of HfO₂ films made with different techniques.

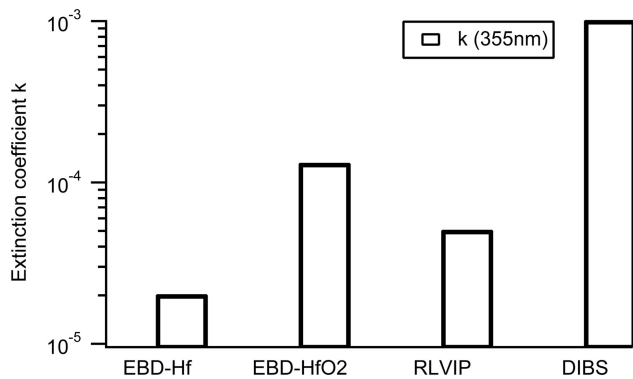


Fig. 3. Extinction coefficient of HfO₂ films made with different techniques.

80 μm × 80 μm. The root mean square values of the roughness are given for all the samples and one bare substrate coming from the same batch in Fig. 4.

A relatively large roughness is found for the EBD samples, since a columnar structure is inherent to the technology. For the RLVIP, the roughness is found similar to the substrate roughness, which is a satisfactory result for an assisted technology. It is also the case for the DIBS layers λ/2 at 355 nm, but the thickest layer exhibits an anomalous high roughness (one possible explanation for this high surface roughness is microcrystallization of the material).

4. Laser Damage Measurements

A. Experiment and Test Procedure

The configuration used for LIDT measurements is described in Fig. 5. The laser source is an injected Nd:YAG laser (Quantel YG 980) with a pulse duration of 11 ns (effective pulse duration at 1/e [19]) and a maximum repetition rate of 10 Hz. The laser can operate at 1064 or 355 nm, with a maximum energy

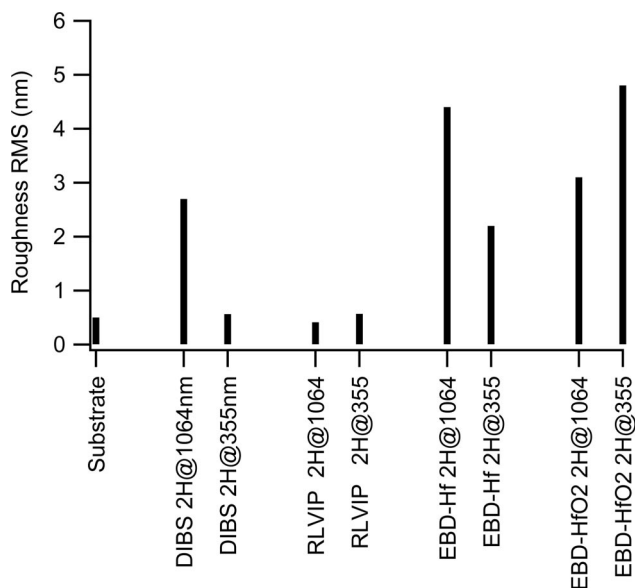


Fig. 4. Roughness of the different samples.

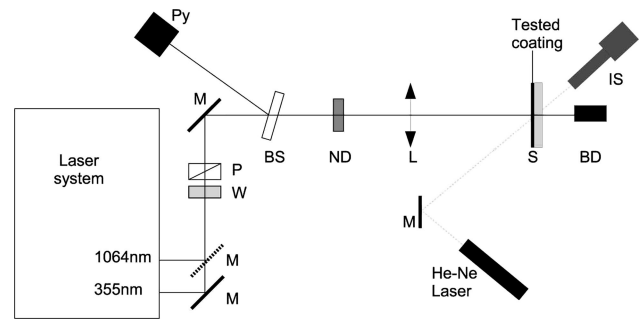


Fig. 5. Experimental setup for laser damage measurements: M, mirror; W, wave plate; P, Glan-laser polarizer; BS, tilted wedge window; Py, pyrometer; NDs, neutral density filters; L, focusing lens; S, sample; BD, beam dump; IS, imaging system.

of 1.5 J at 1064 nm and 450 mJ at 355 nm. It works at a repetition rate of 10 Hz to keep a good stability of energy and beam characteristics. A mechanical shutter permits working in single shot mode. Energy of the beam is controlled with a variable attenuator (half-wave plate and polarizer).

The laser beam (linearly polarized and in normal incidence) is focused on the front face of the coated sample (see Fig. 5) with a plano-convex lens at 1064 nm ($f = 35$ mm) and an objective in the case of 355 nm ($f = 11.5$ mm). The spot size has been measured in the sample plane with a beam analyzer. The spot diameter is 44 μm at 1064 nm and 3 μm at 355 nm (diameter at 1/e).

The damage detection is done by comparing the area before and after irradiation with an imaging system (magnification: 216×) and image processing software. The damage criterion is then any visible modification detected with this system.

For each shot, energy is measured with a pyroelectric detector and recorded. The fluence is then calculated according to the International Organization for Standardization (ISO) standard by using the effective spot size [19].

The LIDT measurement setup is fully automated, which allows one to measure laser damage probabilities with a great number of points. In this study, the damage test procedure one-on-one is used: by counting the number of damaged regions at each fluence F we estimate and plot the damage probability curve $P(F)$. To have good accuracy of the measurement, each curve $P(F)$ is plotted with 1000 data points that involve 20 different fluences and 50 tested regions at each fluence.

B. Results

The test results are plotted in Fig. 6 for 355 nm and Fig. 7 for 1064 nm. The curves in these figures are the fit of the experimental points with a statistical model relying on the hypothesis of defect initiation (see Ref. [12]). The shape and threshold of these curves are linked to the initiator characteristics. However, the analysis of these curves, as well as the scaling of laser-induced damage with spot size, will be reported at a later date since this study is more focused on

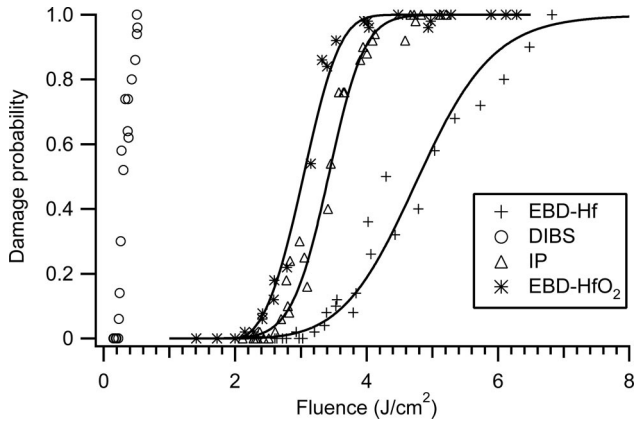


Fig. 6. Laser damage probability curves measured for the different technologies at 355 nm (one-on-one test, 11 ns, 3 μm spot size). Tested samples: DIBS 2H at 355 nm, RLVIP 2H at 355 nm, EBD-Hf 2H at 355 nm, and EBD-HfO₂ 2H at 355 nm. LIDT of the substrate in the same conditions is 18 J/cm².

comparisons of the technologies. The LIDTs of the films, i.e., highest fluence where no damage is observed, are the following:

- EBD-HfO₂: 2.1 J/cm² at 355 nm and 14.5 J/cm² at 1064 nm
- EBD-Hf: 2.8 J/cm² at 355 nm and 3.5 J/cm² at 1064 nm
- RLVIP: 2.3 J/cm² at 355 nm and 15.5 J/cm² at 1064 nm
- DIBS: 0.22 J/cm² at 355 nm and 12 J/cm² at 1064 nm.

One difficulty in laser damage testing is often to compare laser damage performances of a particular material between different testing facilities, where large discrepancies are found between publications. Indeed, the damage threshold can be linked to many factors such as the test procedure, the beam profile,

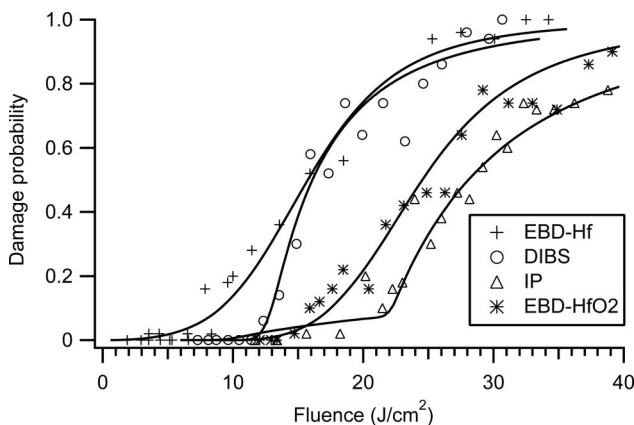


Fig. 7. Laser damage probability curves measured for the different technologies at 1064 nm (one-on-one test, 11 ns, 3 μm spot size). Tested samples: DIBS 2H at 1064 nm, RLVIP 2H at 1064 nm, EBD-Hf 2H at 1064 nm, and EBD-HfO₂ 2H at 1064 nm. LIDT of the substrate in the same conditions is 83 J/cm².

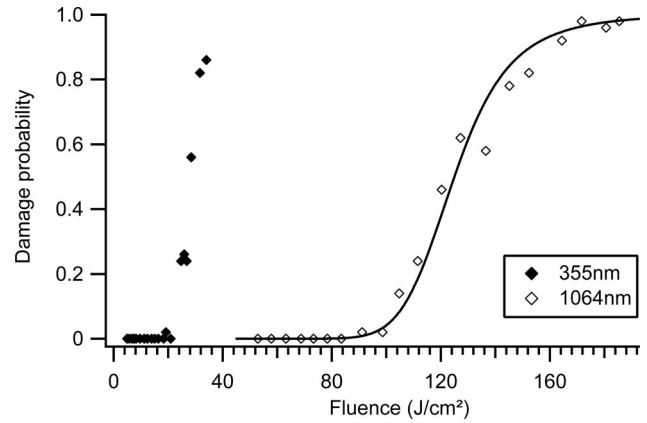


Fig. 8. Laser damage probability curves measured for the substrate.

the wavelength, the pulse profile and duration, and the number of shots. For this reason we also give the LIDT of the substrates (polished, cleaned, and stocked with the coatings substrates) tested in the same experimental conditions shown in Fig. 8 (18 J/cm² at 355 nm and 83 J/cm² at 1064 nm).

5. Discussion

The best threshold in the IR is found for the RLVIP technique, and the worst result is obtained for EBD-Hf. This is quite surprising compared to general results in this field where EBD-Hf is found to be the best technology, particularly at 1064 nm. This indicates that the deposition parameters chosen are far from optimal for the EBD-Hf process and can be further optimized for 1064 nm applications (a high roughness is also found for this film). Nevertheless, in the same conditions a relatively good threshold and very low extinction index are found at 355 nm for this technology.

For the DIBS thin films tested at 355 nm, a very low LIDT is found. This is associated with a high extinction coefficient and a damage morphology evidencing burning and melting of the film. In this case, damage is linked to the high intrinsic absorption level of the film, and thermal melting of the material is the main laser damage mechanism. This can be due to a stoichiometric problem of the film, such as oxygen deficiency, linked to the bombardment process or the relatively low substrate temperature compared to other technologies. Indeed, these parameters critically affect the nucleation, growth, and final composition of the film [8]. The optimization of the DIBS process for UV applications seems delicate: no reports of high LIDT DIBS films in the UV have been published to our knowledge.

As concerns the damage mechanisms involved, except for the DIBS films tested at 355 nm, damage is linked to the defective nature of the films. The laser damage morphologies observed are small pits appearing under the irradiated area. In this work, the tested samples have a half-wave optical thickness, and in this case damage must predominantly occur

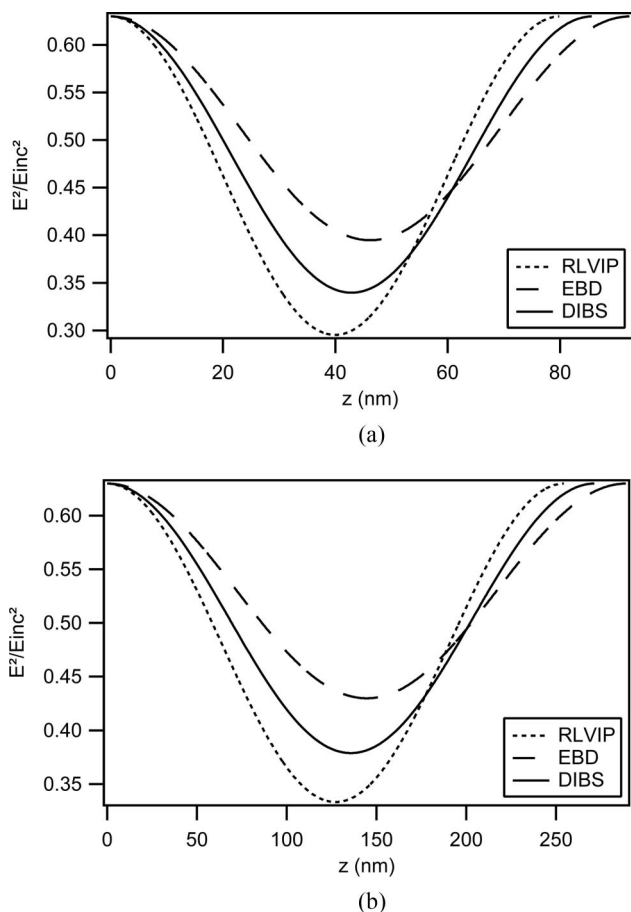


Fig. 9. Standing-wave electric field distribution in the samples. Refractive indices are obtained from Subsection 3.A, and optical thickness is (a) $\lambda/2$ at 355 nm and (b) $\lambda/2$ at 1064 nm.

at or near the interfaces where the standing electric field is maximum (see Fig. 9, where we have plotted the standing electric field distribution for the different samples).

6. Conclusion

Single layers of HfO_2 have been deposited on fused silica with different assisted and nonassisted deposition techniques. The coatings have been characterized with respect to their optical (n , k) and structural properties (surface roughness), as well as the laser-induced damage threshold under 355 and 1064 nm nanosecond laser radiation.

The LIDTs are strongly dependent on the deposition technique but also on the test wavelength. No correlations were found between LIDT at 355 and 1064 nm.

The evaporated films exhibit good thresholds (even if EBD-Hf needs to be optimized at 1064 nm) but suffer of course from high roughness and low density, which prevent their use in very demanding systems.

Eventually, the ion plating technique appears to be the more promising for producing dense films for high power applications at 355 and 1064 nm, since it ex-

hibits simultaneously good optical (n and k) and structural (roughness) properties, combined with a high LIDT. While this technology appears well optimized, further improvement with respect to a lower absorption in the UV region can be achieved for the DIBS process.

Then the next step of our studies will be the production and testing of SiO/HfO_2 multilayer components with the different technologies. For this application, hafnia will be the limiting material. Indeed, silica films exhibit higher LIDT when produced in the same conditions [10].

References

1. R. Chow, S. Falabella, G. E. Loomis, F. Rainer, and C. J. Stolz, "Reactive evaporation of low defect density hafnia," *Appl. Opt.* **32**, 5567–5574 (1993).
2. C. J. Stolz, L. M. Sheehan, M. K. Gunten, R. P. Bevis, and D. Smith, "The advantages of evaporation of hafnium in a reactive environment to manufacture high damage threshold multilayer coatings by electron-beam deposition," *Proc. SPIE* **3338**, 218–324 (1999).
3. M. Alvisi, M. Di Giulio, S. G. Marrone, M. R. Perrone, M. L. Protopapa, A. Valentini, and L. Vasanelli, "HfO₂ films with high laser damage threshold," *Thin Solid Films* **410**, 86–93 (2002).
4. P. André, L. Poupinet, and G. Ravel, "Evaporation and ion assisted deposition of HfO₂ coatings: some key points for high power applications," *J. Vac. Sci. Technol.* **18**, 2372–2377 (2000).
5. R. Thielsch, A. Gatto, J. Heber, and N. Kaiser, "A comparative study of the UV optical and structural properties of SiO₂, Al₂O₃, and HfO₂ single layers deposited by reactive evaporation, ion-assisted deposition, and plasma ion-assisted deposition," *Thin Solid Films* **410**, 86–93 (2002).
6. A. J. Waldorf, J. A. Dobrowolski, B. T. Sullivan, and L. M. Plante, "Optical coatings deposited by reactive ion plating," *Appl. Opt.* **32**, 5583–5593 (1993).
7. H. L. Pulker and M. Reinhold, "Reactive ion plating of optical films," *Int. J. Glass Sci. Technol.* **62**, 100–105 (1989).
8. M. R. Kozłowski, "Damage-resistant laser coatings," in *Thin Films for Optical Systems*, F. Flory, ed. (Marcel Dekker, 1995), pp. 521–549.
9. C. J. Stolz and F. Y. Génin, "Laser resistant coatings," in *Optical Interference Coatings*, N. Kaiser and H. K. Pulker, eds. (Springer, 2003), pp. 309–333.
10. L. Gallais, H. Krol, J. Y. Natoli, M. Commandré, M. Cathelinaud, L. Roussel, M. Lequime, and C. Amra, "Laser damage resistance of silica thin films deposited by electron beam deposition, ion assisted deposition, reactive low voltage ion plating and dual ion beam sputtering," *Thin Solid Films* **515**, 3830–3836 (2007).
11. D. Milam, W. H. Lowdermilk, F. Rainer, J. E. Swain, C. K. Carniglia, and T. Tuttle Hart, "Influence of deposition parameters on laser-damage threshold of silica-tantalum AR coatings," *Appl. Opt.* **21**, 3689–3694 (1982).
12. H. Krol, L. Gallais, M. Commandré, C. Grézes-Besset, D. Torricini, and G. Lagier, "Influence of polishing and cleaning on the laser-induced damage threshold of substrates and coatings at 1064 nm," *Opt. Eng.* **46**, 023402 (2007).
13. M. Cathelinaud, F. Lemarquis, J. Loesel, and B. Cousin, "Metal-dielectric light absorbers manufactured by ion plating," *Proc. SPIE* **5250**, 511–518 (2004).
14. D. L. Wood, K. Nassau, T. Y. Kometai, and D. L. Nash, "Optical properties of cubic hafnia stabilized with yttrium," *Appl. Opt.* **21**, 604–607 (1990).

15. M. Commandré and P. Roche, "Characterization of optical coatings by photothermal deflection," *Appl. Opt.* **35**, 5021–5034 (1996).
16. A. During, C. Fossati, and M. Commandré, "Multiwavelength imaging of defects in ultraviolet optical materials," *Appl. Opt.* **41**, 3118–3126 (2002).
17. L. Gallais and M. Commandré, "Simultaneous absorption, scattering, and luminescence mappings for the characterization of optical coatings and surfaces," *Appl. Opt.* **45**, 1416–1424 (2006).
18. H. A. Macleod, *Thin-Film Optical Filters* (Adam Hilger, 1986).
19. ISO Standard 11254–1, "Determination of laser-damage threshold of optical surfaces. Pt. 1: 1-on-1 test" (International Organization for Standardization, 2000).